Induction of Caspase-Dependent Apoptosis in Cultured Cells by the Avian Coronavirus Infectious Bronchitis Virus

C. LIU, H. Y. XU, AND D. X. LIU*

Institute of Molecular Agrobiology, The National University of Singapore, Singapore 117406, Singapore

Avian coronavirus infectious bronchitis virus (IBV) is the causative agent of chicken infectious bronchitis, an acute, highly contagious viral respiratory disease. Replication of IBV in Vero cells causes extensive cytopathic effects (CPE), leading to destruction of the entire monolayer and the death of infected cells. In this study, we investigated the cell death processes during acute IBV infection and the underlying mechanisms. The results show that both necrosis and apoptosis may contribute to the death of infected cells in lytic IBV infection. Caspase-dependent apoptosis, as characterized by chromosomal condensation, DNA fragmentation, caspase-3 activation, and poly(ADP-ribose) polymerase degradation, was detected in IBV-infected Vero cells. Addition of the general caspase inhibitor z-VAD-FMK to the culture media showed inhibition of the hallmarks of apoptosis and increase of the release of virus to the culture media at 16 h postinfection. However, neither the necrotic process nor the productive replication of IBV in Vero cells was severely affected by the inhibition of apoptosis. Screening of 11 IBV-encoded proteins suggested that a 58-kDa mature cleavage product could induce apoptotic changes in cells transiently expressing the protein. This study adds one more example to the growing list of animal viruses that induce apoptosis during their replication cycles.

Apoptosis, or programmed cell death, is a highly conserved, tightly controlled self-destruction process to ablate damaged and neoplastic cells in multicellular organisms. Upon activation of apoptosis by monitoring extracellular or intracellular death signals, cells display characteristically morphological changes, including chromatin condensation, plasma membrane blebbing, cell shrinkage, and fragmentation into membrane-bound bodies (4). The central players in apoptosis are a family of cysteine-dependent aspartate-directed proteinases, termed caspases, which catalyze key steps in the death pathway by cleavage of substrates at specific sites containing aspartic acid (9, 10). The nuclear condensation is the consequence of DNA fragmentation manifested by the characteristic oligonucleosome-sized DNA ladder, mediated by the activation of a caspase-dependent endonuclease, the DNA fragmentation factor (9). Apoptosis also represents an important antivirus defense mechanism of the host cell, and viruses have evolved strategies to counteract and regulate apoptosis in order to maximize the production of virus progeny and promote the spread of virus progeny to neighboring cells. In recent years, many viruses in different families, including two coronaviruses, have been found to induce apoptosis during their infection cycles (28, 31, 32).

Coronavirus is the largest RNA virus identified so far. It has a positive-sense, single-stranded RNA genome of 27 to 30 kb and typically contains four structural proteins, the spike (S), nucleocapsid, membrane (M), and envelope (E) proteins. A fifth protein, the hemagglutinin-esterase glycoprotein, is found in some but not all coronaviruses as short spikes. Coronavirus also encodes several nonstructural proteins by subgenomic

mRNAs and two large polyproteins by mRNA 1. The two polyproteins are processed by viral proteinases to generate more than 10 mature cleavage products (39). The avian coronavirus *Infectious bronchitis virus* (IBV) is a prototype of the *Coronaviridae* family. It is the etiological agent of infectious bronchitis, an acute disease impairing the respiratory and urogenital tracts of chickens (15, 29). After adaptation to a cell culture system (e.g., Vero cells), IBV undergoes a cytolytic life cycle. A hallmark of IBV infection of cultured cells is the formation of syncytial cells, which spread quickly from an original virus-infected cell to the surrounding cells. The syncytium is progressively destroyed, and the cells round up and detach from the substratum, concomitant with the secretion of virions. Although extensive studies on viral replication, subgenomic RNA transcription, posttranslational processing of mRNA 1-encoded polyproteins, and the assembly of virions have been carried out in recent years, the mechanisms that control how and when infected cells die in the acute IBV infection are not fully understood.

Two coronaviruses have been shown to induce apoptosis. Infection of four different cell lines with the porcine coronavirus transmissible gastroenteritis virus induced caspase-dependent apoptosis, possibly through cellular oxidative stress (11, 36). Infection of cultured macrophages and other cell lines with the murine coronavirus mouse hepatitis virus was also shown to induce apoptosis, which could be triggered by overexpression of the E protein (2, 6), which suggests that coronavirus E protein may be proapoptotic. In this report, we demonstrate that caspase-dependent apoptosis is induced in Vero cells during acute IBV infection. Our data also showed that overexpression of a 58-kDa protein encoded in the open reading frame (ORF) 1b region triggered apoptosis, suggesting that it may be a virus-derived death signal, though some other source of proapoptotic signals could not be rule out. Controversial results regarding the proapoptotic role of the E protein

* Corresponding author. Mailing address: Institute of Molecular Agrobiology, 1 Research Link, The National University of Singapore, Singapore 117406, Singapore. Phone: 65-872-7000. Fax: 65-872-7007. E-mail: liudx@ima.org.sg.

were generated. The protein induced more dead cells when coexpressed in Vero cells with the green fluorescent protein (GFP). However, it did not induce apoptotic changes when overexpressed in BHK cells via a Sindbis virus expression vector. In fact, it seems that the protein may be able to inhibit apoptosis induced by Sindbis virus proteins in BHK cells. Furthermore, inhibition of IBV-induced apoptosis by the general caspase inhibitor z-VAD-FMK marginally affects the replication and accumulation of IBV. This finding suggests that other death processes, such as necrosis, may also contribute to the death of IBV-infected cells.

MATERIALS AND METHODS

Virus and cells. The egg-adapted Beaudette strain of IBV (ATCC VR-22) was obtained from the American Type Culture Collection and was adapted to Vero cells as described previously (22). Virus stock was prepared by infection of Vero cells with 0.1 PFU of virus per cell and incubation at 37°C for 32 h. After freezing and thawing for three times, cell lysates were aliquoted and stored at −80°C as virus stocks. The virus stocks were sonicated for 1 min with a 15-s interval before used. Titers of the virus stocks were determined by plaque assay on Vero cells, and 2 PFU of virus per cell was used to infect Vero cells in all experiments.

Vero cells were maintained in Dulbecco modified Eagle medium supplemented with 10% bovine calf serum and grown at 37°C in 5% CO_2.

DNA transfection. Sixty to 80% confluent monolayers of cells grown on 35-mm-diameter dishes (Falcon) were transfected with 5 μg of plasmid DNA (purified by using Qiagen plasmid Midi kits) mixed with Lipofectin transfection reagent according to the instructions of the manufacturer (Life Technologies). After incubation at 37°C in 5% CO_2 for the appropriate amount of time, the cells were analyzed further as indicated for each experiment.

Transient expression of proteins in a Sindbis virus expression system. For expression of IBV proteins in a Sindbis virus expression system, cDNA fragments encoding the proteins were cloned into pSinRep5 (Invitrogen) under the control of a promoter for subgenomic RNA transcription. RNA transcripts (recombinant RNA) containing ORFs coding for the nonstructural proteins of Sindbis virus and the protein of interest were generated in vitro by using SP6 polymerase. Meanwhile, RNA transcripts (helper RNA) containing ORFs coding for the structural proteins of Sindbis virus were prepared in the same way, using DH(26S) as the template. Equal amounts of the recombinant and helper RNAs were mixed and transfected into BHK cells by electroporation. The cells were incubated at 37°C in 5% CO_2 for 24 to 48 h before being harvested for further analysis. The supernatant contains the recombinant Sindbis pseudovirions, which can be used to express the protein of interest by infection of fresh cells.

SDS-PAGE and Western blotting. Sodium dodecyl sulfate-polyacrylamide gel electrophoresis (SDS-PAGE) of viral polypeptides was performed on SDS–7.5 to 17.5% polyacrylamide gels. Proteins separated by SDS-PAGE were electroblotted onto a nitrocellulose membrane in transfer buffer (0.5 mM Tris-HCl, 0.2 M glycine, 20% methanol) at 20 V for 40 min, using a semidry transfer cell (Bio-Rad). The membrane was blocked in TBST (20 mM Tris-HCl [pH 7.5], 150 mM NaCl, 0.05% Tween 20) containing 3% nonfat milk at room temperature overnight and then blotted with the first antibody in TBST buffer for 1 h. After being washed with TBST for three times, the membrane was transferred to TBST buffer containing 1:2,000-diluted secondary antibody for 30 min with gentle agitation, and proteins were detected by using an ECL+Plus Western blotting detection kit (Amersham Pharmacia Biotech).

Analysis of apoptosis. Low-molecular-weight nuclear DNA was isolated as described by Saeki et al. (33). Briefly, the attached and floating cells were harvested and treated with lysis buffer (0.6% SDS, 0.1% EDTA [pH 8.0]). After incubation at room temperature for 10 min, 21 μl of 5 M NaCl was added to the lysates, which were then incubated at 4°C for at least 8 h and centrifuged at 15,000 rpm at 4°C for 20 min. The supernatant was treated first with heat-inactivated RNase A (1 mg/ml) at 45°C for 90 min and then with proteinase K (200 μg/ml) for 60 min, followed by phenol extraction and ethanol precipitation. One-third of the DNA sample was analyzed on 2% agarose gel, and the size of the oligonucleosomal DNA fragment was measured by comparison with the 1-kb markers.

The terminal deoxynucleotidyltransferase-mediated dUTP-biotin nick end labeling (TUNEL) assay was performed with a DeadEnd colorimetric apoptosis detection kit according to the protocol of the manufacturer (Promega). Briefly, cells were fixed with paraformaldehyde and permeabilized with Triton X-100 at room temperature. After equilibration, specimens were overlaid with 25 μM

biotinylated nucleotide and 25 U of terminal deoxynucleotidyltransferase and incubated at 37°C for 60 min, the reaction was stopped by adding 2× SSC (1× SSC is 0.15 M NaCl plus 0.015 M sodium citrate), and the endogenous peroxidase was blocked by incubation of the specimens with 0.3% hydrogen peroxide for 3 min. The fragmented DNA was detected by binding the horseradish peroxidase-labeled streptavidin to the biotinylated nucleotides and visualizing by using the peroxidase substrate hydrogen peroxide and the stable chromogen diaminobenzidine.

PCR. Complementary DNA templates for PCR were prepared from purified IBV virion RNA by using a first-strand cDNA synthesis kit (Boehringer Mannheim). Amplification of the template DNAs with appropriate primers was performed with *Pfu* DNA polymerase (Stratagene) under the standard buffer conditions with 2 mM $MgCl_2$. The reaction conditions used were 30 cycles of 95°C for 45 s, *x*°C for 45 s, and 72°C for *x* min. The annealing temperature (*x*°C) and the extension time (*x* min) were adjusted according to the melting temperatures of the primers used and the lengths of PCR fragments synthesized.

Construction of plasmids. Two recombinant Sindbis virus constructs expressing E and 58-kDa proteins were constructed by cloning an *Nhe*I- and *Sma*I-restricted fragment into *Xba*I- and *Stu*I-digested pSinRep5, giving pSinRepE and pSinRep58K. The two *Nhe*I- and *Sma*I-digested fragments, which cover the IBV sequences from nucleotides 24209 to 24794 and 16930 to 18495, respectively, were obtained by digestion of pIBVE and pIBV1b6 with the two restriction enzymes. Both pIBVE and pIBV1b6 were generated by cloning *Nco*I- and *Bam*HI-digested PCR fragments into *Nco*I- and *Bam*HI-digested pKT0 (20). Sequences of the primers used for generating the PCR fragment containing nucleotides 24209 to 24928 (a *Bam*HI restriction site is at position 24794) are 5′-GATTGTTCAGG<u>CCATGG</u>TGAATTTATTGAA-3′ and 5′-GCACCATTG GCACACTC-3′; sequences of the primers used for generating the PCR fragment containing nucleotides 16930 to 18495 are 5′-ACAAGTC<u>CCATGGG</u>TA CAGGTT-3′ and 5′-TATT<u>GGATCC</u>TACTGGACTGGAG-3′ (the underlining indicates the restriction site introduced by each primer). Plasmid pSinRepGFP, which expresses GFP, was constructed by cloning an *Nhe*I- and *Sma*I-digested fragment from pEGFP-C1 (Clontech) into pSinRep5.

RESULTS

Morphological and biochemical evidence of apoptosis induced in Vero cells by IBV infection. IBV replication in Vero cells resulted in typical cytopathic effects (CPE), i.e., rounding up and fusion of infected cells to form multinucleated giant syncytia, detachment of infected cells from the culture dish, and eventually cell lysis and death. The mechanisms that lead to the death of IBV-infected cells are not fully understood. Careful examination of infected cells by light microcopy showed characteristic signs of apoptosis during the infection process. As shown in Fig. 1, a drastic loss of cell volume leading to cell shrinkage accompanied the formation of syncytia, and prevalent cytoplasmic blebbing became visible shortly thereafter. Nuclear staining of infected cells with the membrane-permeable DNA-binding dye Hoechst 33342 showed gradually morphological changes of the nuclei. In mock-infected cells, the nuclei remained uniformly stained without condensation at 36 h postinfection (Fig. 1). In IBV-infected cells, slight condensation of the nuclei with heterogeneous staining patterns appeared at 12 to 16 h postinfection, almost coincident with the appearance of CPE (Fig. 1). The nuclei became apparently distorted and fragmented (i.e., pyknotic) at 36 h postinfection (Fig. 1). These results indicate that apoptosis may be triggered in Vero cells during IBV infection.

We then performed two biochemical assays to ascertain whether the morphological changes observed in IBV-infected Vero cells were due to the induction of apoptosis. First, the low-molecular-weight genomic DNA extracted from IBV-infected Vero cells at 8, 24, and 48 h postinfection was analyzed on a 2% agarose gel. As shown in Fig. 2a, a canonic oligonucleosome-sized DNA ladder was observed in cells harvested at

M-36 h pi   I-16 h pi   I-36 h pi
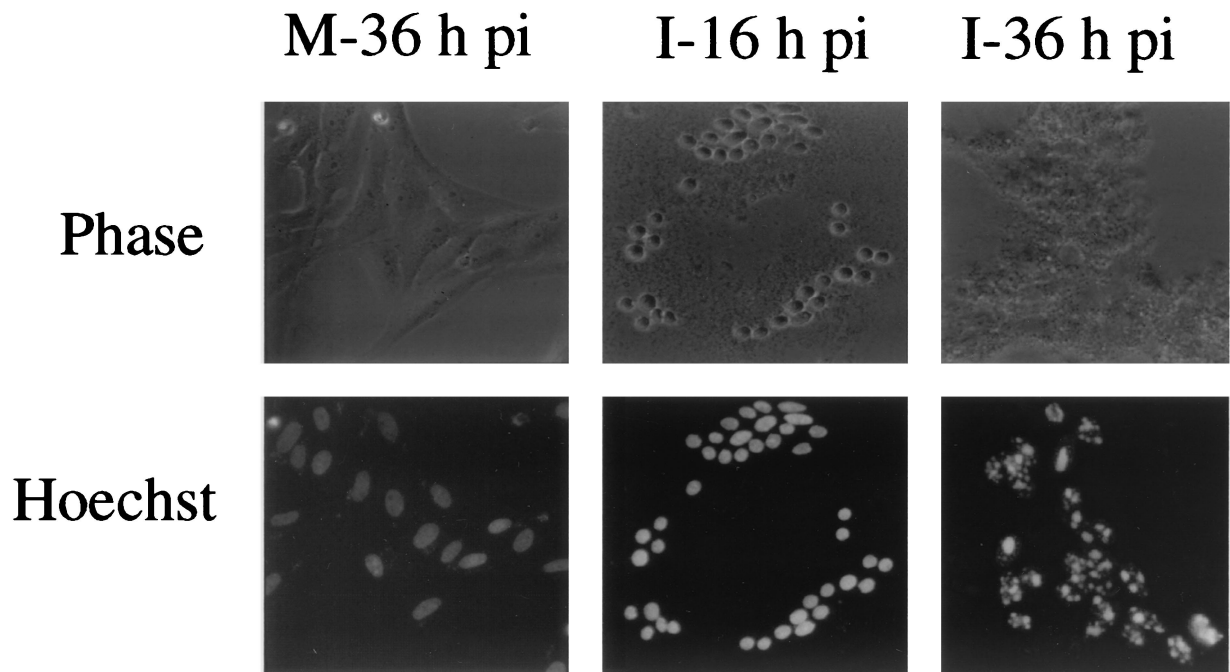
Phase

Hoechst

FIG. 1. Morphological changes in IBV-infected Vero cells. Cells were mock (M) or IBV (I) infected, stained with Hoechst 33342 at 16 and 36 h postinfection (pi), and viewed in a light microscope. Phase, phase-contrast images; Hoechst, nuclear staining.

48 h postinfection, confirming that DNA fragmentation was induced by IBV infection (lane 7). No obvious DNA fragmentation was observed in mock- and IBV-infected cells harvested at 8 and 24 h postinfection (Fig. 2a, lanes 2 to 6). Second, nuclear TUNEL staining was performed on mock- and IBV-infected Vero cells at 8, 24, and 48 h postinfection. As the

TUNEL assay could distinguish apoptotic cells undergoing DNA fragmentation by adding labeled nucleotides to the fragmented DNA ends, cells even at early stages of apoptosis could be visualized by horseradish peroxidase colorimetric reaction. As shown in Fig. 2b, TUNEL signal-positive cells began to appear at 8 h postinfection. The number of positive cells in-

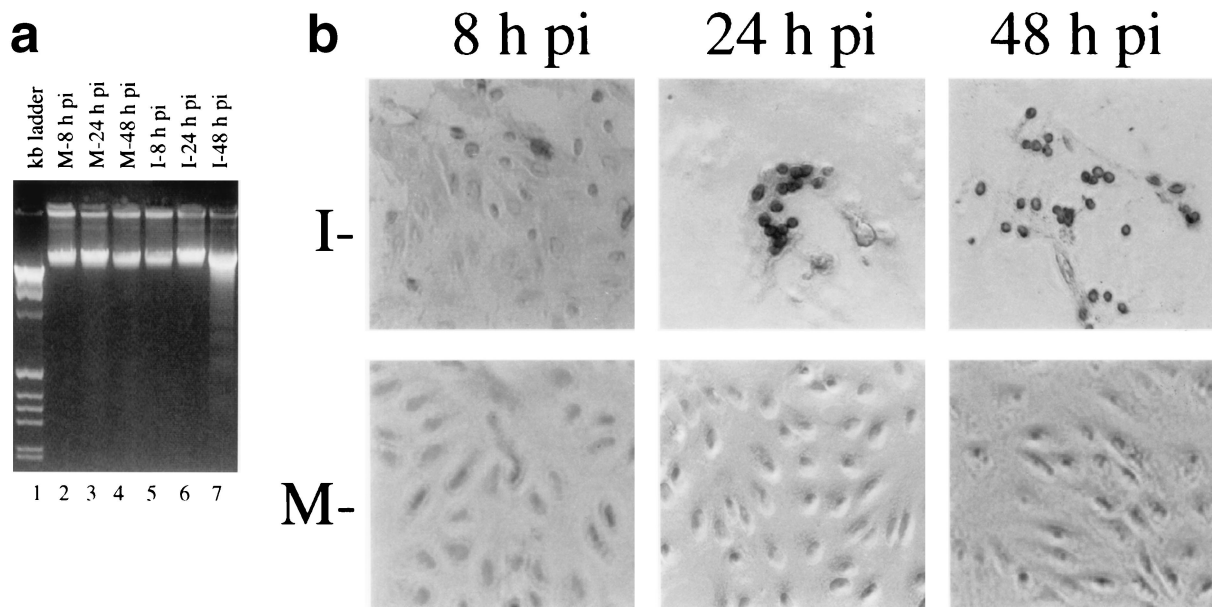**a**   **b**   8 h pi   24 h pi   48 h pi

I-

M-

FIG. 2. (a) DNA fragmentation assay of IBV-infected Vero cells. Low-molecular-weight DNA was isolated from mock (M)- (lanes 2 to 4) and IBV (I)-infected Vero cells harvested at 8 (lane 5), 24 (lane 6), and 48 (lane 7) h postinfection (pi) and analyzed on a 2% agarose gel. The 1-kb ladder DNA markers (lane 1) were purchased from Gibco BRL (Life Technologies). (b) TUNEL assay of mock- and IBV-infected cells at 8, 24, and 48 h postinfection.
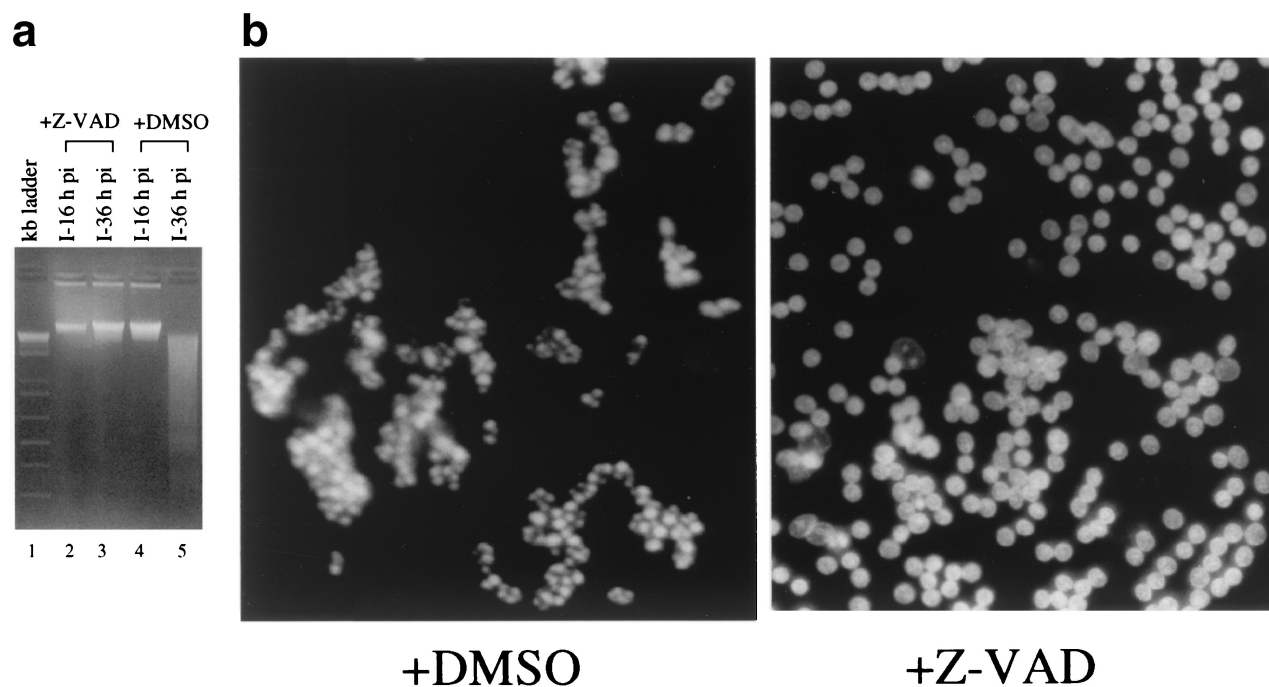
FIG. 3. (a) Effects of z-VAD-FMK on DNA fragmentation in IBV-infected Vero cells. Cells were infected with 2 PFU of IBV per cell in the presence of DMSO (20 μl/ml) (lanes 4 and 5) or z-VAD-FMK (20 μg/ml) (lanes 2 and 3). Low-molecular-weight DNA was isolated from IBV-infected (I) Vero cells at 16 (lanes 2 and 4) and 36 (lanes 3 and 5) h postinfection and analyzed on a 2% agarose gel. The 1-kb ladder DNA markers (lane 1) were purchased from Gibco BRL (Life Technologies). (b) Effects of z-VAD-FMK on morphological changes of nuclei of IBV-infected Vero cells. Cells were infected with 2 PFU of IBV per cell in the presence of DMSO (20 μl/ml) or z-VAD-FMK (20 μg/ml). The nuclei were stained with Hochest 33342 at 36 h postinfection and viewed with a light microscope.

creased at 24 h postinfection (Fig. 2b). The positive nuclei were found mainly in cells that formed syncytia, indicating that apoptosis was tightly associated with productive virus replication. At 48 h postinfection, the majority of infected cells were detached from the culture dish. The few cells remaining attached showed positive TUNEL staining (Fig. 2b). Few if any positive signals were found in mock-infected cells (Fig. 2b).

Inhibition of IBV-induced apoptosis but not productive replication of IBV in Vero cells by the general caspase inhibitor z-VAD-FMK. To test if the apoptotic changes observed in IBV-infected Vero cells were caspase dependent, the general caspase inhibitor z-VAD-FMK was added to the culture media of infected cells. z-VAD-FMK is a specific tetrapeptide pseudosubstrate for several caspases, including caspase-3, which could irreversibly block the caspase proteolytic cascade (27). As shown in Fig. 3a, the DNA ladder was once again detected in the low-molecular-weight DNA preparation extracted from virus-infected cells harvested at 36 h postinfection (lane 5). In the presence of 20 μg of z-VAD-FMK per ml, however, no DNA ladder was detected in infected cells harvested at 36 h postinfection (Fig. 3a, lane 3). These results demonstrate that z-VAD-FMK could effectively inhibit IBV-induced apoptosis and suggest that IBV-induced apoptosis may be caspase dependent.

The effects of z-VAD-FMK on IBV-induced CPE in Vero cells were assessed. In the presence of 20 μg of z-VAD-FMK per ml, chromatin condensation and nuclear fragmentation were remarkably reduced, as shown by Hoechst 33342 staining (Fig. 3b). The nuclei of infected cells showed slight condensation

and were heterogeneously stained but remained intact up to 36 h postinfection (Fig. 3b). However, the infected cells continued to form syncytia, lose volume, and disintegrate in the presence of z-VAD-FMK (data not shown). The finding suggests that the morphological changes of the nuclei and the cleavage of genomic DNA in the late cytolytic cycle may be caspase-dependent apoptotic processes that can be separated from other virus-promoted events that lead to the destruction of infected cells.

The effects of apoptosis on the replication of IBV were assayed by comparing virus titers in the presence and absence of 20 μg of z-VAD-FMK per ml. As dimethyl sulfoxide (DMSO), the solvent used to dissolve z-VAD-FMK, appears to affect the viability of IBV, virus titers produced in the presence of DMSO were generally 1.5 to 3 logs lower than those in the absence of DMSO. In the presence of z-VAD-FMK at 16 h postinfection, the titers of viable viruses released into the media and remaining in the cells were 1.5×10^3 and 4.5×10^4 PFU/ml, respectively, compared to 2.5×10^2 and 3.5×10^4 PFU/ml in the absence of z-VAD-FMK. At 36 h postinfection, the titers of viable viruses remaining in the cells were 1.5×10^3 in the presence and 1.5×10^2 in the absence of z-VAD-FMK. No virus was detected in the media harvested at this time point, possibly due to long exposure of the virus to DMSO. These results may indicate that inhibition of apoptosis has differential effects on the replication and release of IBV in cell culture at different stages of infection; however, the dramatic inhibitory effect of DMSO on the viability of IBV may obscure the interpretation of these data.
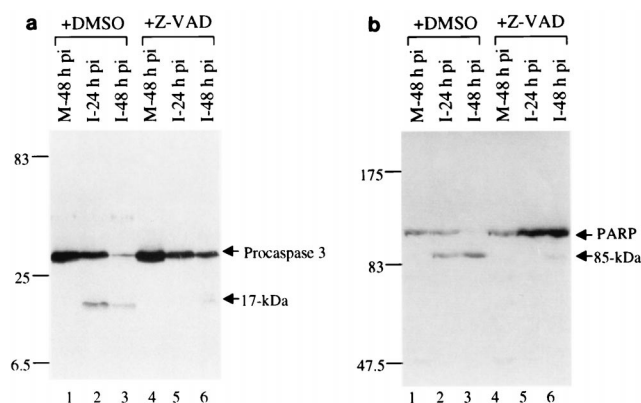
FIG. 4. (a) Western blotting analysis of caspase-3 in IBV-infected Vero cells. Cells were mock (M) or IBV (I) infected in the presence of DMSO (20 μl/ml) (lanes 1 to 3) or z-VAD-FMK (20 μg/ml) (lanes 4 to 6) and harvested at 24 and 48 h postinfection (pi). Caspase-3 was analyzed by separation of total proteins on SDS–17.5% polyacrylamide gels, transfer to a nitrocellular membrane, and blotting with a rabbit anti-caspase-3 polyclonal antibody (PharMingen). The protein was detected by using an ECL+Plus Western blotting detection kit (Amersham Pharmacia Biotech). Numbers on the left indicate molecular masses in kilodaltons. (b) Western blotting analysis of PARP in IBV-infected Vero cells. Cells were mock or IBV infected in the presence of DMSO (20 μl/ml) (lanes 1 to 3) or z-VAD-FMK (20 μg/ml) (lanes 4 to 6) and harvested at 24 and 48 h postinfection. PARP was analyzed by separation of total proteins on SDS–7.5% polyacrylamide gels, transfer to a nitrocellular membrane, and blotting with an anti-PARP 3 monoclonal antibody (PharMingen).

Activation of caspase-3 and cleavage of poly (ADP-ribose) polymerase (PARP) during IBV-induced apoptosis in Vero cells. The observation that z-VAD-FMK could inhibit IBV-induced apoptosis suggests that activation of caspases may occur during the infection process. We tested the activation of caspase-3 by Western blotting analysis of IBV-infected cells by using a commercially available anti-caspase-3 polyclonal antibody (PharMingen). As caspase-3 is one of the main effector caspases and is activated in response to both intracellular and extracellular death signals, its activation would provide additional evidence that IBV infection triggers apoptosis. For this purpose, Vero cells were mock or IBV infected, harvested at 24 and 48 h postinfection, and then subjected to Western blotting analysis. To minimize the potential effects of serum variation in the culture media on cell survival, the inoculum used for mock infection was prepared from uninfected cells in the same way as the virus stock. Western blotting analysis of total cell lysates prepared from mock-infected cells harvested at 48 h postinoculation showed the presence of a polypeptide with an apparent molecular mass of 32 kDa (Fig. 4a, lanes 1 and 4), representing procaspase-3. In addition to the 32-kDa procaspase-3, a polypeptide of 17 kDa, representing a cleavage form of procaspase-3, was detected in virus-infected cells harvested at both 24 and 48 h postinfection (Fig. 4a, lanes 2 and 3). These results confirm that cleavage of procaspase-3 occurred in IBV-infected Vero cells. Addition of z-VAD-FMK to the culture media blocked the cleavage of procaspase-3 into the activated form. In the presence of 20 μg of z-VAD-FMK per ml, only the 32-kDa procaspase-3 was detected in virus-infected cells harvested at 24 h postinfection (Fig. 4a, lane 5).

Trace amounts of the 17-kDa cleavage form were detected in cells harvested at 48 h postinfection (Fig. 4a, lane 6).

We next analyzed cleavage of one of the typical substrates of caspases, PARP. Consistent with the activation of pro-caspase-3, Western blotting analysis of samples prepared from mock-infected cells harvested at 48 h postinoculation detected only the full-length, 116-kDa PARP (Fig. 4b, lanes 1 and 4). Cleavage of the 116-kDa protein into an 85-kDa form was observed in virus-infected cells harvested at both 24 and 48 h postinfection (Fig. 4b, lanes 2 and 3). Once again, addition of z-VAD-FMK to the culture media blocked cleavage of the 116-kDa PARP into the 85-kDa form. As can be seen, only the 116-kDa PARP was detected in virus-infected cells harvested at 16 h postinfection in the presence of 20 μg of z-VAD-FMK per ml (Fig. 4b, lane 5). Trace amounts of the 85-kDa form were detected in cells harvested at 48 h postinfection (Fig. 4b, lane 6).

Induction of apoptosis by overexpression of a 58-kDa protein encoded in the ORF 1b region of the IBV genome. After confirming that IBV infection induces apoptosis in Vero cells, the permissive cell line for IBV infection, we then tried to screen for IBV-encoded proteins (virus-encoded proapoptotic proteins) that may be responsible for the induction of apoptosis. As IBV is a large RNA virus with a genome of 27.6 kb in length, manipulation of the genome by reverse genetics has proved to be an intimidating task. The strategy of overexpressing individual viral proteins by using transient expression systems was employed to screen for IBV-encoded proapoptotic proteins.

The initial screening was carried out either by expression of IBV proteins as a fusion with GFP or by coexpression of IBV proteins with GFP. The IBV proteins included in this screening are three structural (S, M, and E) and two nonstructural (5a and 5b) encoded proteins by mRNA 5 (19) and six mature cleavage products (33-, 24-, 10-, 58-, 39-, and 35-kDa proteins) (18, 21, 22, 26) from mRNA 1-encoded polyproteins. After transfection of cells with individual constructs, the cells were stained with Hoechst 33342 at 24 to 36 h posttransfection. The total GFP-positive cells and the number of cells with fragmented or condensed nuclei among the GFP-positive cells were counted, and the percentage of dead cells was calculated. The results of this initial screening showed that expression of the structural protein E and the 58-kDa protein as GFP fusion constructs induced 1.5- and 3-fold, respectively, more dead cells than did the GFP control at 24 h posttransfection (data not shown). Expression of other proteins did not lead to significantly more dead cells than in the control in this screening.

The regions that code for the E and 58-kDa proteins were then cloned into a dicistronic construct in which the viral sequences were placed under the control of the internal ribosome entry element of encephalomyocarditis virus. The viral proteins and GFP were therefore expressed as separate proteins in the same cells after transfection. Upon transfection of Vero cells with the constructs, the nuclei of some GFP-positive cells exhibited apoptotic changes. In each experiment, 200 to 500 GFP-positive cells and cells with apoptotic changes among the GFP-positive cells were counted, and the percentage of dead cells was calculated. The same experiment was repeated four times for each construct. The results (Table 1) showed that significantly more dead cells were induced in cells express-

TABLE 1. Percentage of dead cells induced by IBV E and 58-kDa protein

Protein	Mean % ± SE ($n = 4$)	
	24 h	48 h
GFP	22.10 ± 4.21	49.90 ± 7.62
E	40.12 ± 3.23	78.72 ± 2.60
58 kDa	52.21 ± 4.50	82.84 ± 3.75

ing the E protein than in the control ($P < 0.01$). Induction of dead cells by overexpression of the 58-kDa protein was also significantly higher than in the GFP only control ($P < 0.01$) (Table 1).

To gain biochemical evidence that overexpression of the E and 58-kDa proteins induced apoptotic changes, cDNA fragments coding for the 58-kDa protein, E, and GFP were cloned into a Sindbis virus expression vector and expressed in BHK cells. The GFP construct was used to monitor transfection efficiency and as a negative control. The transfected cells were harvested for Western blotting and DNA fragmentation assays when more than 85% of cells transfected with the helper RNA and RNA coding for GFP showed fluorescence. Figure 5a shows the results of Western blotting analysis. As can be seen, efficient expression of the E and 58-kDa proteins was observed upon transfection of BHK cells with the helper RNA and the corresponding constructs (Fig. 5a, lanes 3 and 6). Analysis of the low-molecular-weight genomic DNA extracted from the
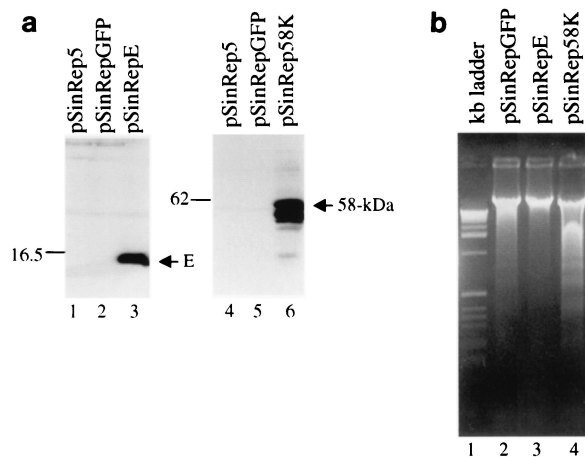

FIG. 5. (a) Western blotting analysis of the E and 58-kDa proteins overexpressed in BHK cells in a Sindbis virus expression system. Cells were transfected with RNA transcribed from plasmids as indicated above each lane by electroporation and were harvested at 48 h post-transfection. Gel electrophoresis of the total proteins was performed on SDS–17.5% (lanes 1 to 3) and 10% (lanes 4 to 6) polyacrylamide gels, respectively. The proteins were transferred to nitrocellular membranes, blotted with rabbit anti-E and anti-58-kDa protein polyclonal antibodies, respectively, and detected by using an ECL+Plus Western blotting detection kit (Amersham Pharmacia Biotech). Numbers on the left indicate molecular masses in kilodaltons. (b) Induction of DNA fragmentation in BHK cells by overexpression of the 58-kDa protein in a Sindbis virus expression system. Cells were transfected with RNA transcribed from plasmids as indicated above each lane by electroporation. Low-molecular-weight DNA was isolated at 48 h post-transfection and analyzed on a 2% agarose gel. The 1-kb ladder DNA markers (lane 1) were purchased from Gibco BRL (Life Technologies).

transfected cells showed the detection of an oligonucleosome-sized DNA ladder in cells expressing the 58-kDa protein (Fig. 5b, lane 4). Trace amounts of fragmented DNA were also detected in cells expressing GFP (Fig. 5b, lane 2), as Sindbis virus structural proteins could induce apoptosis (14). However, no sign of the formation of a DNA ladder was observed in cells expressing E (Fig. 5b, lane 3).

DISCUSSION

Virus-induced cell death is a complex and important aspect of the pathogenesis of virus infection. During the past 10 years, the ability of numerous viruses to elicit or inhibit apoptosis either directly or indirectly during their replication cycles has been demonstrated (28, 31, 32). In this report, we show that infection of Vero cells with the coronavirus IBV induces caspase-dependent apoptosis. Characteristically morphologic and biochemical features of apoptosis, such as blebbing of the plasma membrane, chromatin condensation, fragmented nuclei, and nicked DNA, were detected during IBV infection. The chromatin condensation and pyknosis of nuclei could be inhibited by the general caspase inhibitor z-VAD-FMK. In the presence of the caspase inhibitor, however, the infected cells continued to lose volume and eventually died of necrosis, indicating that cell death induced by IBV may recruit two biochemically distinct death processes, apoptosis and necrosis. By expressing individual viral proteins in cultured cell lines, we provided further evidence that a 58-kDa protein encoded in the ORF 1b region may contribute to the induction of apoptosis during IBV infection.

Necrosis and apoptosis are two distinct forms of cell death. Necrosis is a caspase-independent process, lacking DNA fragmentation. In this death process, the cytoplasmic substances do not package into apoptotic bodies, resulting in leakage of intracellular contents to neighboring tissue and therefore stimulating an inflammatory reaction. This could be caused by the destructive effects of syncytium formation, virus morphogenesis, and secretion. During virus infection, both necrosis and apoptosis may be attributed to the death of infected cells (7, 23). For example, replication of bovine viral diarrhea virus was not affected by antioxidant that protected cells from virus-induced apoptosis at late stages of infection (35). Both CPE and necrosis were also not affected by the inhibition of apoptosis (35). Similar phenomena also occurred in poliovirus (1). However, in the presence of z-VAD-FMK, cell shrinkage and cytoplasmic blebbing were still observed in IBV-infected cells. The reason for this observation remains elusive. Some researchers suggest that cytoplasmic blebbing and cell volume loss could be the consequence of caspase-dependent cleavage of the actin-severing protein gelsolin (16). Others argued that blebbing was a caspase-independent process because many cells blebbed for days when caspase activities were apparently inhibited (24, 25). It is therefore possible that in the presence of a caspase inhibitor, IBV-infected cells lose volume and die of apoptotic mechanisms independent of caspases rather than necrosis.

It is apparent that apoptosis may represent a by-product of the action of virus replication. On the one hand, apoptosis may facilitate the release of virus progeny and help virus to evade the immune surveillance by attenuating inflammation (34). On

the other hand, premature apoptosis, most likely evoked by host defense mechanisms, aborts virus infection and therefore limits virus productivity and infectivity. The intricate balance between life and death of infected cells must be regulated by viral products or by interaction between virus and host to ensure a successful infection cycle. In recent years, it has been documented that numerous viruses encode pro- and antiapoptotic proteins, such as BRLF-1 and LMP-1 of Epstein-Barr virus, Crm of poxvirus, p35 of baculovirus, and E1A of human adenovirus (32, 37). These products may be involved in the regulation of apoptosis induced by these viruses, therefore facilitating viral production and dissemination in virus-infected cells or tissues. In addition, virus-induced apoptosis involves composite interaction between viral and host factors. One example is the activation of the double-stranded RNA protein kinase (PKR) pathway by RNA viruses, which in turn activates apoptosis and influences the fate of infected cells (5, 38). PKR is an interferon-inducible kinase mediating the antiviral actions by autophosphorylation and phosphorylation of eIF2a after activated by double-stranded RNA (8). Overexpression of PKR could induce apoptosis (17). It was hypothesized that PKR may serve as a novel apoptotic checkpoint monitoring abnormal translational initiation to restrict virus production (3, 13). During the replication of RNA viruses, PKR may be activated. To investigate if excess PKR may be activated during IBV infection, Western blotting analysis of PKR in IBV-infected cells harvested at different times of postinfection was carried out. No obvious increase of the phosphorylation of PKR at the time of apoptosis detected was observed (data not shown), ruling out the possibility that activation of PKR may contribute significantly to the induction of apoptosis during IBV infection.

The observation that the 58-kDa protein may be a proapoptotic protein suggests that synthesis of certain viral proteins may be a trigger that elicits apoptosis in IBV-infected cells. We are not certain whether these proteins may induce apoptosis by interacting or interfering with the classical apoptotic pathways. Other two potential factors related to viral protein synthesis may also contribute to the induction of apoptosis in IBV-infected cells. The first is the fusion of infected cells mediated by the expression of the S protein. As dramatic rearrangement of cellular structures occurred during the fusion process, cells may undergo apoptosis in response to this stimulus. However, overexpression of the S protein induces massive cell fusion but not apoptosis, suggesting that induction of cell fusion alone cannot trigger the death pathway. The second potential factor that may trigger apoptosis is the massive production of viral membrane proteins, which may alter the intracellular structures of the infected cells. One example is the coronavirus E protein. Expression of E could induce formation of tubular structures in the endoplasmic reticulum (30), which might serve as an endoplasmic reticulum stress signal to trigger apoptosis. In this study, however, we show that IBV E could not induce the formation of DNA ladders in BHK cells when overexpressed in a Sindbis virus expression system (Fig. 5b). On the contrary, it seems to be able to inhibit DNA fragmentation induced by the Sindbis virus structural proteins (Fig. 5b). Further investigations are required to understand the controversial observations of the IBV E protein in inducing and inhibiting apoptosis.

Expression of the 58-kDa protein in IBV-infected cells has not been fully characterized. Proteolytic mapping of the 1a/b polyprotein encoded by mRNA 1 showed the identification of two QS dipeptide bonds, encoded by nucleotides 16929 to 16934 and 18492 to 18497, respectively, in the ORF 1b region. The two sites flank the 58-kDa protein-encoding region (22). Cleavage at these positions by the 3C-like proteinase would result in the formation of a protein with a calculated molecular mass of 58 kDa. The protein has recently been identified in virus-infected cells (unpublished observations). Further characterization of the protein in virus-infected cells and deletion analysis of its proapoptotic domain are under way.

Our results suggest that apoptosis renders certain but not dramatic effects on the replication and release of IBV in the cell culture system. This is understandable, as apoptosis is mainly induced at late stages of IBV infection, and the adverse effects of apoptosis on IBV replication would be avoided. However, as one of the main advantages of apoptotic cell death for virus infectivity is to facilitate the spread of virus progeny to the neighboring cells and to minimize the inflammatory reaction evoked by virus-infected cells on the host, we expect that IBV-induced apoptosis would facilitate virus infection in animals. Other studies also suggest that viruses and other intracellular parasites may pirate apoptosis to help their dissemination in vivo and evasion of host defense mechanisms (12, 32).

REFERENCES

1. **Agol, V. I., G. A. Belov, K. Bienz, D. Egger, M. S. Kolesnikova, N. T. Raikhlin, L. I. Romanova, E. A. Smirnova, and E. A. Tolskaya.** 1998. Two types of death of poliovirus-infected cell: caspase involvement in the apoptosis but not cytopathic effect. Virology **252:**343–353.
2. **An, S., C.-J. Chen, X. Yu, J. L. Leibowitz, and S. Makino.** 1999. Induction of apoptosis in murine coronavirus-infected cultured cells and demonstration of E protein as an apoptosis inducer. J. Virol. **73:**7853–7859.
3. **Anderson, P.** 1997. Kinase cascade regulating entry into apoptosis. Microbiol. Mol. Biol. Rev. **61:**33–46.
4. **Arends, M., and A. Wellie.** 1991. Apoptosis: mechanism and roles in pathology. Int. Rev. Exp. Pathol. **32:**223–254.
5. **Balachandran, S., P. C. Roberts, T. Kipperman, K. N. Bhalla, R. W. Compans, D. R. Archer, and G. N. Barber.** 2000. Alpha/beta interferons potentiate virus-induced apoptosis through activation of the FADD/caspase-8 death signaling pathway. J. Virol. **74:**1513–1523.
6. **Belyavskyi, M., E. Belyavskaya, G. A. Levy, and J. L. Leibowitz.** 1998. Coronavirus MHV-3-induced apoptosis in macrophages. Virology **250:**41–49.
7. **Columbano, A.** 1995. Cell death: current difficulties in discriminating apoptosis from necrosis in the context of pathological processes in vivo. J. Cell Biol. **58:**181–190.
8. **Cosentino, G., S. Venkatesan, F. Serluca, S. Green, M. Mathews, and N. Sonenberg.** 1995. Double-stranded-RNA-dependent protein kinase and TAR RNA-binding protein form homo- and heterodimers in vivo. Proc. Natl. Acad. Sci. USA **92:**9445–9449.
9. **Cryns, V., and J. Yuan.** 1998. Proteases to die for. Genes Dev. **12:**1551–1570.
10. **Earnshaw, W. C., L. M. Martins, and S. H. Kaufmann.** 1999. Mammalian caspases: structure, activations, and functions during apoptosis. Annu. Rev. Biochem. **68:**383–424.
11. **Eleouet, J.-F., S. Chilmonczyk, L. Besnardeau, and H. Laude.** 1998. Transmissible gastroenteritis coronavirus induces programmed cell death in infected cells through a caspase-dependent pathway. J. Virol. **72:**4918–4924.
12. **Freire-de-Lima, C. G., D. O. Nascimento, M. B. Soares, P. T. Bozza, H. C. Castro-Faria-Neto, F. G. de Mello, G. A. DosReis, and M. F. Lopes.** 2000. Uptake of apoptotic cells drives the growth of a pathogenic trypanosome in macrophages. Nature **403:**199–203.
13. **Jagus, R. J. B., and G. N. Barber.** 1999. PKR, apoptosis and cancer. Int. J. Biochem. Cell Biol. **31:**123–138.
14. **Jan, J.-T., and D. E. Griffin.** 1999. Induction of apoptosis by Sindbis virus

occurs at cell entry and does not require virus replication. J. Virol. 73:10296–10302.

15. King, D. J., and D. Cavanagh. 1991. Infectious bronchitis, p. 471–484. *In* B. W. Calnek, H. J. Barnes, C. W. Beard, W. M. Reid, and H. W. Yoder, Jr. (ed.), Disease of poultry, 9th ed. Iowa State University Press, Ames, Iowa.

16. Kothakota, S., T. Azuma, C. Reinhard, A. Klippel, J. Tang, K. Chu, T. J. McGarry, M. W. Kirschner, K. Koths, D. J. Kwiatkowski, and L. T. Williams. 1997. Caspase-3-generated fragment of gelsolin: effector of morphological change in apoptosis. Science 278:294–298.

17. Lee, S., and M. Esteban. 1994. The interferon induced double-stranded RNA activated protein kinase induces apoptosis. Virology 199:491–496.

18. Lim, K. P., L. F. P. Ng, and D. X. Liu. 2000. Identification of a novel cleavage activity of the first papain-like proteinase domain encoded by open reading frame 1a of the coronavirus avian infectious bronchitis virus and characterization of the cleavage products. J. Virol. 74:1674–1685.

19. Liu, D. X., and S. C. Inglis. 1992. Identification of two new polypeptides encoded by mRNA5 of the coronavirus infectious bronchitis virus. Virology 186:342–347.

20. Liu, D. X., I. Brierley, K. W. Tibbles, and T. D. K. Brown. 1994. A 100K polypeptide encoded by open reading frame (ORF) 1b of the coronavirus infectious bronchitis virus is processed by ORF1a products. J. Virol. 68:5772–5780.

21. Liu, D. X., H. Y. Xu, and T. D. K. Brown. 1997. Proteolytic processing of the coronavirus infectious bronchitis virus 1a polyprotein: identification of a 10 kDa polypeptide and determination of its cleavage sites. J. Virol. 71:1814–1820.

22. Liu, D. X., S. Shen, H. Y. Xu, and S. F. Wang. 1998. Proteolytic mapping of the coronavirus infectious bronchitis virus 1b polyprotein: evidence for the presence of four cleavage sites of the 3C-like proteinase and identification of two novel cleavage products. Virology 246:288–297.

23. Majno, G., and I. Joris. 1995. Apoptosis, oncosis and necrosis: an overview of cell death. Am. J. Pathol. 146:3–15.

24. McCarthy, N. J., M. K. B. Whyte, C. S. Gilbert, and G. I. Evan. 1997. Inhibition of Ced-3/ICE-related proteases does not prevent cell death induced by oncogenes, DNA damage or the Bcl-2 homologue Bak. J. Cell Biol. 136:215–227.

25. Mills, J. C., N. L. Stone, J. Erhardt, and R. N. Pittman. 1998. Apoptotic membrane blebbing is regulated by myosin light chain phosphorylation. J. Cell Biol. 140:627–636.

26. Ng, L. F. P., and D. X. Liu. 1998. Identification of a 24 kDa polypeptide processed from the coronavirus infectious bronchitis virus 1a polyprotein by the 3C-like proteinase and determination of its cleavage sites. Virology 243:388–395.

27. Nicholson, D. W., and N. A. Thornberry. 1997. Caspases: killer proteases. Trends Biochem. Sci. 22:299–306.

28. O'Brien, V. 1998. Viruses and apoptosis. J. Gen. Virol. 79:1833–1845.

29. Picault, J. P., P. Drouin, M. Guittet, G. Bennejean, J. Protais, R. L'Hospitalier, J. P. Gillet, J. Lamande, and A. L. Bachelier. 1986. Isolation, characterization and preliminary cross protection studies with a new pathogenic avian infectious bronchitis virus (strain PL-84084). Avian Pathol. 15:367–383.

30. Raamsman, M. J., J. K. Locker, A. de Hooge, A. A. F. de Vries, G. Griffiths, H. Vennema, and P. J. M. Rottier. 2000. Characterization of the coronavirus mouse hepatitis virus strain A59 small membrane protein E. J. Virol. 74:2333–2342.

31. Razvi, E. S., and R. M. Welsh. 1995. Apoptosis in viral infections. Adv. Virus Res. 45:1–60.

32. Roulston, A., R. C. Marcellus, and P. E. Branton. 1999. Virus and apoptosis. Annu. Rev. Microbiol. 53:577–628.

33. Saeki, K., A. Yuo, M. Kato, M. Kohei, M. Yazaki, and F. Takaku. 1997. Cell density-dependent apoptosis in HL-60 cells, which is mediated by an unknown soluble factor, is inhibited by transforming growth factor 1 and overexpression of Bcl-2. J. Biol. Chem. 272:20003–20010.

34. Savill, J., V. Fadok, P. Henson, and C. Haslett. 1993. Phagocyte recognition of cells undergoing apoptosis. Immunol. Today 14:131–136.

35. Schweizer, M., and E. Peterhans. 1999. Oxidative stress in cells infected with bovine viral diarrhea virus: a crucial step in the induction of apoptosis. J. Gen. Virol. 80:1147–1155.

36. Sirinarumitr, T., J. P. Kluge, and P. S. Paul. 1998. Transmissible gastroenteritis virus induced apoptosis in swine testes cell cultures. Arch. Virol. 143:2471–2485.

37. Teodoro, J. G., and P. E. Branton. 1997. Regulation of apoptosis by viral gene products. J. Virol. 71:1739–1746.

38. Yeung, M. C., D. L. C. Randell, E. Camantigue, and A. S. Lau. 1999. Inhibitory role of the host apoptogenic gene PKR in the establishment of persistent infection by encephalomyocarditis virus in U937 cells. Proc. Natl. Acad. Sci. USA 96:11860–11865.

39. Ziebuhr, J., E. J. Snijder, and A. E. Gorbalenya. 2000. Virus-encoded proteinases and proteolytic processing in the Nidovirales. J. Gen. Virol. 81:853–879.